

Supplementary information

One-dimensional molecular nanostructures interacting with two-dimensional metal.

Pavel Kocán,^{*,†} Barbara Pieczyrak,[‡] Soshiro Umachi,[¶] Martin Cigánek,[§] Pavel Sobotík,[†] Ivan Ošťádal,[†] Leszek Jurczyszyn,[‡] Jozef Krajčovič,[§] and Kazuyuki Sakamoto[¶]

[†]*Faculty of Mathematics and Physics, Charles University, Prague, Czech Republic*

[‡]*Institute of Experimental Physics, University of Wrocław, Wrocław, Poland*

[¶]*Department of Applied Physics, Osaka University, Osaka 565-0871, Japan*

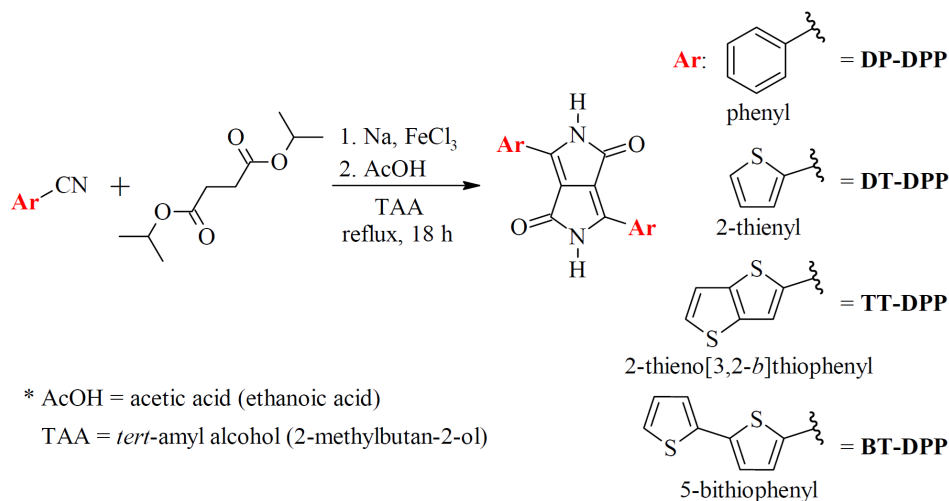
[§]*Brno University of Technology, Faculty of Chemistry, Materials Research Centre,
Purkyňova 118, 612 00, Brno, Czech Republic*

E-mail: pavel.kocan@mff.cuni.cz

Phone: +420 22191 2349

Synthesis of DPP derivatives

Target 4 DPP derivatives were synthesized according to the known general procedure through condensation of aryl nitrile derivatives with succinic acid esters, the so-called *Succinic method* (Ref. 1). Sodium (~1.3 equiv.) was dissolved in *tert*-amyl alcohol (TAA, 0.6M solution of aryl nitrile) with the addition of a catalytic amount of iron^(III) chloride and heated to reflux under argon atmosphere. After the dissolution of all sodium, there was added in one portion 1.0 equiv. of aryl nitrile (Ar-CN) and the reaction mixture was stirred at reflux for 30 min.

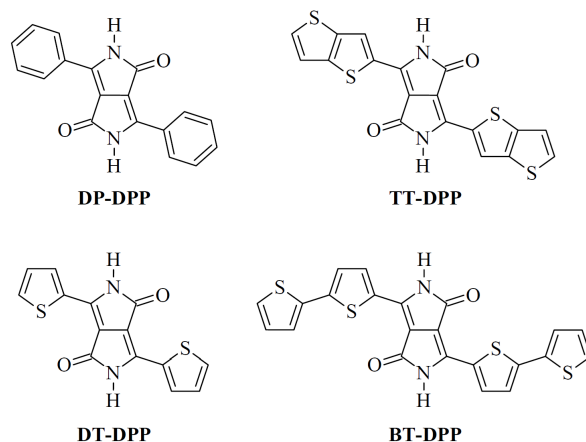


Scheme S1: Synthesis of the final DPP derivatives by the *Succinic method*.

Then, 0.65 equiv. of diisopropyl succinate dissolved in TAA (approx. 2M solution) was gradually added dropwise for 4 h and the mixture was stirred at reflux for 18 h. After that, protolysis was performed by addition of diluted acetic acid to the reaction mixture cooled to 20 °C. The mixture was refluxed for 6 h, and then the heterogenic mixture was filtered while hot and the filter cake was washed with hot water and isopropyl alcohol. The crude product was refluxed in methanol for 1 h and, after that, it was filtered while hot to get pure DPP product.

DP-DPP: Intense red powder (23.5 g, yield 52%). Melting point 371 °C (lit. 372 °C) (Ref. 2). ¹H NMR (300 MHz, DMSO-*d*₆, ppm): δ = 11.29 (s, 2H), 8.43 (m, 4H), 7.55 (m, 6H). Anal. calcd. for C₁₈H₁₂N₂O₂: C 74.99 %, H 4.20 %, N 9.72 %; Found: C 74.63 %, H 3.98 %, N 10.02 %.

DT-DPP: Dark purple powder (27.5 g, yield 59%). Melting point >380 °C (lit. >360 °C) (Ref. 3). ¹H NMR (300 MHz, DMSO-*d*₆, ppm): δ = 11.21 (s, 2H), 8.20 (d, *J* = 3.0 Hz, 2H), 7.93 (d, *J* = 3.1 Hz, 2H), 7.31–7.27 (m, 2H). Anal. calcd. for C₁₄H₈N₂O₂S₂: C 55.98 %, H 2.68 %, N 9.33 %, S 21.35 %; Found: C 55.62 %, H 2.37 %, N 9.51 %, S 21.02 %.



Scheme S2: Overview of 4 synthesized and studied final DPP derivatives.

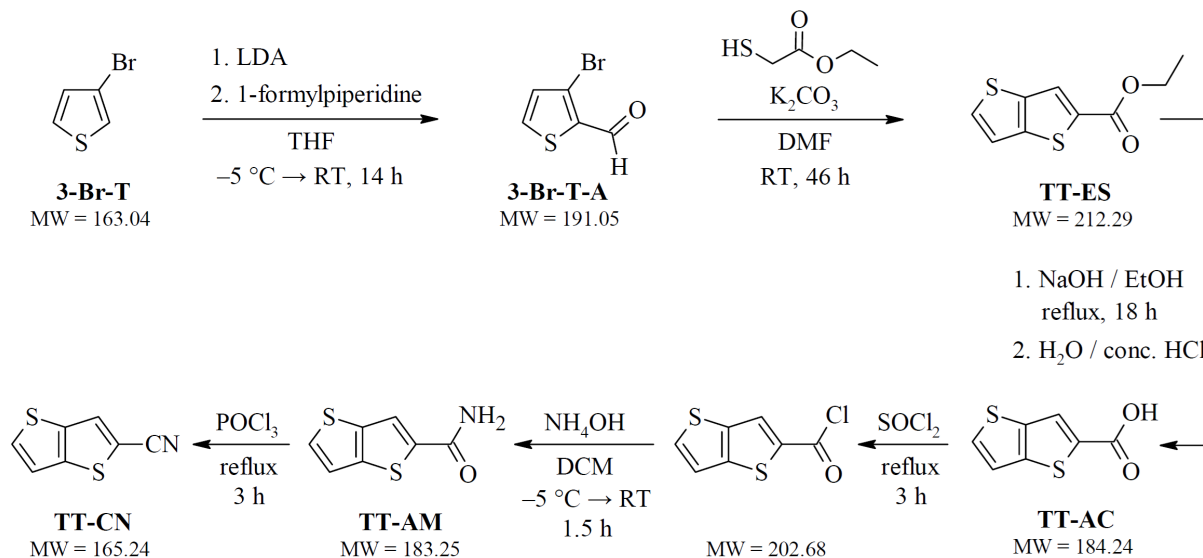
TT-DPP: Dark blue-black powder (0.44 g, yield 41 %). Melting point $>380^{\circ}\text{C}$ (lit.-). ^1H NMR (500 MHz, DMSO- d_6 , ppm): $\delta = 11.22$ (s, 2H), 8.19 (s, 2H), 7.92 (d, $J = 4.2$ Hz, 2H), 7.28 (d, $J = 3.6$ Hz, 2H). Anal. calcd. for $\text{C}_{18}\text{H}_8\text{N}_2\text{O}_2\text{S}_4$: C 52.41 %, H 1.95 %, N 6.79 %, S 31.09 %; Found: C 52.17 %, H 2.02 %, N 6.83 %, S 30.62 %.

BT-DPP: Dark purple-black powder (1.94 g, yield 35 %). Melting point $>380^{\circ}\text{C}$ (lit.-). ^1H NMR (500 MHz, DMSO- d_6 , ppm): $\delta = 11.24$ (s, 2H), 8.91 (d, $J = 4.1$ Hz, 2H), 7.33 (dd, $J = 10.4$; 4.6 Hz, 6H), 7.09 (dd, $J = 5.1$; 3.6 Hz, 2H). Anal. calcd. for $\text{C}_{22}\text{H}_{12}\text{N}_2\text{O}_2\text{S}_4$: C 56.87 %, H 2.60 %, N 6.03 %, S 27.61 %; Found: C 57.00 %, H 2.62 %, N 6.09 %, S 28.00 %.

Sodium and iron^(III) chloride (anhydrous, $>97\%$) were purchased from *Sigma-Aldrich, Inc.* tert-Amyl alcohol (p.a., 98%), acetic acid (p.a, glacial 99.8%), isopropyl alcohol (p.a, 99.8%) and methanol (p.a., 99.8%) were purchased from *PENTA*, spol. s r.o. Diisopropyl succinate (p.a., 95%) was purchased from *Synthesis, a.s.*

Aryl nitriles (Ar-CN) used for the DPPs synthesis: benzonitrile (anhydrous, $\geq 99\%$) and 2-thiophenecarbonitrile (99%) were purchased from *Sigma-Aldrich, Inc.* Thieno[3,2-*b*]thiophene-2-carbonitrile (**TT-CN**) was prepared according to the following procedure:

3-bromothiophene (**3-Br-T**, 9.50 g, 58.27 mmol) was dissolved in anhydrous THF (50 mL) under argon atmosphere, and the reaction mixture was cooled to -5°C and stirred for 10 min.



Scheme S3: Used synthetic route leading from 3-bromothiophene (**3-Br-T**) to thieno[3,2-b]thiophene-2-carbonitrile (**TT-CN**).

After that, 1.05 equiv. of LDA (2M, 30.59 mL, 61.18 mmol) was added dropwise to the mixture and it was stirred at RT for 1.5 h. Following that 1.05 equiv. of 1-formylpiperidine (7.76 mL/7.91 g, 69.92 mmol) was added and the reaction mixture was stirred at RT for 18 h. Then, the reaction was quenched with the addition of a saturated NH₄Cl solution (10 mL), and extraction was performed. The reaction mixture was washed with diethyl ether (2×120 mL), and the collected organic phases were washed with distilled water (3×250 mL), finally with brine (200 mL) and then dried over anhydrous Na₂SO₄ and filtered through filter aid (Celite). After removal of the solvent under vacuum, the obtained crude mixture was purified by silica gel chromatography eluting with petroleum ether/toluene 4:1 (v/v) to get pure product 3-bromothiophene-2-carbaldehyde (**3-Br-T-A**, RF = 0.18, eluent: petroleum ether/toluene 4:1) as a lightly yellowish liquid (8.46 g, yield 76 %). ¹H NMR (300 MHz, CDCl₃, ppm): δ = 9.96 (s, 1H), 7.68 (dd, *J* = 5.0; 1.2 Hz, 1H), 7.13 (dd, *J* = 5.0; 1.3 Hz, 1H).

3-Br-T-A (8.05 g, 42.14 mmol) and potassium carbonate (~2.0 equiv., 11.65 g, 84.29 mmol) were stirred in anhydrous DMF (60 mL) under argon atmosphere at RT for

1 h. After that, 1.2 equiv. of ethyl thioglycolate (5.55 mL/6.08 g, 50.59 mmol) was added to the mixture and stirred at RT for another 45 h. Then, the reaction was quenched with the addition of distilled water (100 mL), and the reaction mixture was washed with ethyl acetate (2×80 mL). The collected organic phases were washed with distilled water (3×250 mL), finally with brine (200 mL) and then dried over anhydrous Na₂SO₄ and filtered through filter aid (Celite). After removal of the solvent under vacuum, the obtained crude mixture was purified by silica gel chromatography eluting with ethyl acetate to obtain pure product ethyl thieno[3,2-*b*]thiophene-2-carboxylate (**TT-ES**, RF = 0.40, eluent: ethyl acetate) as a light yellow liquid (5.73 g, yield 64 %). ¹H NMR (500 MHz, CDCl₃, ppm): δ = 7.98 (s, 1H), 7.56 (d, *J* = 5.1 Hz, 1H), 7.26 (d, *J* = 5.2 Hz, 1H), 4.35 (q, *J* = 6.9 Hz, 2H), 1.39 (t, *J* = 7.0 Hz, 3H).

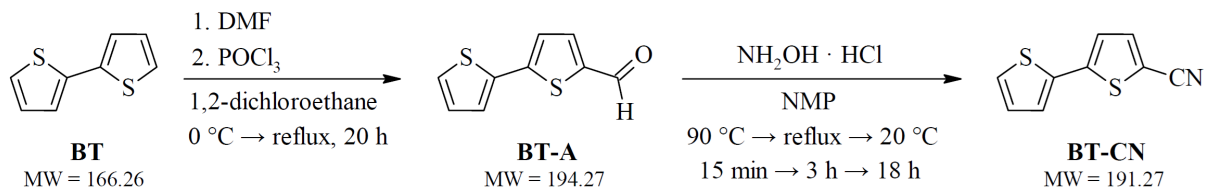
TT-ES (5.65 g, 26.61 mmol) was dissolved in a mixture of ethanol (120 mL) and NaOH (3 equiv., 3.20 g, 80.01 mmol). The reaction mixture was stirred at reflux for 18 h. After that, the reaction mixture was poured into distilled water (150 mL) and conc. hydrochloric acid (58 mL) was added dropwise. The formed precipitate was filtered off and washed with distilled water (3×60 mL). The crude product obtained was crystallized using *n*-heptane to afford pure product thieno[3,2-*b*]thiophene-2-carboxylic acid (**TT-AC**) as a yellow-beige solid material (4.02 g, yield 82 %). Melting point 219 °C (lit. 221–222 °C)(Ref. 4). ¹H NMR (500 MHz, CDCl₃, ppm): δ = 8.11 (s, 1H), 7.65 (d, *J* = 5.2 Hz, 1H), 7.33 (d, *J* = 5.2 Hz, 1H). Anal. calcd. for C₇H₄O₂S₂: C 45.63 %, H 2.19 %, N 0 %, S 34.81 %; Found: C 45.24 %, H 2.31 %, N 0 %, S 35.12 %.

TT-AC (2.11 g, 11.45 mmol) was stirred in 60 equiv. of thionyl chloride (50 mL, 686 mmol) at reflux for 3 h. Unreacted thionyl chloride was then distilled off from the reaction mixture, and the beige-brown solid material was dissolved in DCM (25 mL). The reaction mixture was cooled to –5 °C, ammonium hydroxide (35 mL) in DCM (35 mL) was added dropwise, and the mixture was stirred at RT for 1.5 h. The obtained milky-white needles were filtered off, and the filter cake was washed with distilled water (3×90 mL), then

with DCM (3×70 mL). After precise drying in a vacuum desiccator (at 80 °C for 90 min), product thieno[3,2-*b*]thiophene-2-carboxamide (**TT-AM**) was obtained as a white-beige solid material (1.64 g, yield 78 %), which was used in the next reaction step without further purification. ¹H NMR (500 MHz, DMSO-*d*₆, ppm): δ = 8.08 (s, 2H), 7.82 (d, *J* = 5.2 Hz, 1H), 7.49 (d, *J* = 5.1 Hz, 2H).

TT-AM (1.62 g, 8.84 mmol) was stirred in 30 equiv. of phosphoryl trichloride (24.80 mL, 265 mmol) at reflux for 3 h. Unreacted phosphoryl trichloride was then distilled off from the reaction mixture, and DCM (50 mL) was added to the solid residue. After that, cold distilled water (150 mL) was added dropwise to the mixture and extraction was performed. The reaction mixture was washed with DCM (3×20 mL). The collected organic phases were then washed with saturated NaHCO₃ solution (150 mL), followed by distilled water (2×150 mL), finally with brine (150 mL) and then dried over anhydrous Na₂SO₄ and filtered through filter aid (Celite). After removal of the solvent under vacuum, the obtained crude mixture was purified by silica gel chromatography eluting with toluene/DCM 1:1 (v/v) to get pure product thieno[3,2-*b*]thiophene-2-carbonitrile (**TT-CN**, RF = 0.75, eluent: toluene/DCM 4:1) as a beige-yellow solid material (1.24 g, yield 85 %). ¹H NMR (300 MHz, CDCl₃, ppm): δ = 7.77 (s, 1H), 7.70 (d, *J* = 5.2 Hz, 1H), 7.29 (d, *J* = 5.2 Hz, 1H).

2,2'-Bithiophene-5-carbonitrile (**BT-CN**) was prepared according to the following procedure:



Scheme S4: Used synthetic route leading from 2,2'-bithiophene (**BT**) to 2,2'-bithiophene-5-carbonitrile (**BT-CN**).

2,2'-Bithiophene (**BT**, 10.0 g, 60.15 mmol) was dissolved in anhydrous 1,2-dichloroethane (150 mL) under argon atmosphere. After the dissolution of material, 0.98 equiv. of anhy-

drous DMF (4.56 mL/ 4.31 g, 58.94 mmol) was added in one portion and the reaction mixture was purged with argon for 30 min. Then, the reaction mixture was cooled to 0 °C, and at this temperature, it was added dropwise (for 20 min) 0.98 equiv. of POCl₃ (5.51 mL/9.04 g, 58.94 mmol) and the mixture was heated to reflux and stirred for 20 h. After that, the reaction mixture was cooled to 20 °C and poured into saturated NaHCO₃ solution (300 mL). Solid residues were dissolved in DCM (50 mL) and poured into the previous solution. The obtained two-phase mixture was transferred to a separating funnel, and extraction was performed (DCM/distilled water). The organic phase was finally washed with brine and dried over anhydrous Na₂SO₄ and filtered through filter aid (Celite). Concentrated obtained crude mixture was purified by silica gel chromatography eluting with toluene to get pure product 2,2'-bithiophene-5-carbaldehyde (**BT-A**, RF = 0.38, eluent: toluene) as a beige solid material (10.1 g, yield 87 %). Melting point 56 °C (lit. 57–58 °C)(Ref. 5). ¹H NMR (300 MHz, CDCl₃, ppm): δ = 9.85 (s, 1H), 7.66 (d, *J* = 3.9 Hz, 1H), 7.34 (m, 2H), 7.25 (d, *J* = 3.9 Hz, 1H), 7.05 (t, *J* = 4.3 Hz, 1H).

BT-A (10.08 g, 51.89 mmol) was dissolved in anhydrous NMP (140 mL) under argon atmosphere, and the reaction mixture was heated to 90 °C and stirred for 15 min. After that, 1.50 equiv. of hydroxylamine hydrochloride (5.41 g, 77.83 mmol) was added piece by piece to the mixture and it was stirred at reflux for 3 h. Then, the reaction mixture was cooled to 20 °C and stirred overnight. After that, the reaction mixture was poured into distilled water (380 mL) and stirred for 45 min. Then, diethyl ether (150 mL) was added to the mixture and extraction was performed. The aqueous phase was washed with diethyl ether (2×90 mL), and the collected organic phases were washed with distilled water (3×250 mL), finally with brine (200 mL) and then dried over anhydrous Na₂SO₄ and filtered through filter aid (Celite). After removal of the solvent under vacuum, the obtained crude mixture was purified by silica gel chromatography eluting with toluene to get pure product 2,2'-bithiophene-5-carbonitrile (**BT-CN**, RF = 0.78, eluent: toluene) as a beige crystal material (8.74 g, yield 88 %). Melting point 73 °C (lit. 74–75 °C)(Ref. 6). ¹H NMR (300 MHz, CDCl₃, ppm): δ = 7.53

(d, $J = 3.9$ Hz, 1H), 7.36 (dd, $J = 5.1; 1.1$ Hz, 1H), 7.29 (dd, $J = 3.7; 1.1$ Hz, 1H), 7.15 (d, $J = 3.9$ Hz, 1H), 7.08 (dd, $J = 5.1; 3.6$ Hz, 1H).

1,2-dichloroethane (anhydrous, 99.8%), 1-formylpiperidine (99%), 2,2'-bithiophene (99%), 3-bromothiophene (97%), ammonium hydroxide (28%), ammonium chloride (anhydrous, powder, 99.99%), Celite (R566, Supelco, pH > 8.5), diethyl ether (99.5%), ethyl thioglycolate (97%), lithium diisopropylamide solution (LDA, 2.0M in THF/heptane), phosphoryl trichloride (99.99%), potassium carbonate (anhydrous, 99.99%), tetrahydrofuran (THF, anhydrous, $\geq 99.9\%$) and thionyl chloride ($\geq 99\%$) were purchased from *Sigma-Aldrich, Inc.* Dichloromethane (DCM, p.a., 99.8%), ethanol (p.a., 96%), ethyl acetate (p.a., 99%), hydrochloric acid (p.a., 35%), *n*-heptane (p.a., 99%), petroleum ether (p.a., 40–65 °C), sodium sulfate (p.a., anhydrous) and toluene (p.a., 99%) were purchased from *PENTA, spol. s r.o.* *N,N*-dimethylformamide (DMF, anhydrous, 99.8%) was purchased from *Fisher Scientific, spol. s r.o.* Sodium hydrogen carbonate (p.a.), sodium hydroxide (p.a.) and sodium chloride (p.a.) were purchased from *Lach-Ner, spol. s r.o.*

Periodicity determination and analysis of bonding energies

DFT has been used to analyze bonding energies of selected DPP molecules on the Si(111)-In($\sqrt{7} \times \sqrt{3}$) surface. In the case of DP-DPP we extracted an approximate superstructure from STM images (see Fig.S1 a) as matrix ((6,2),(-1,13)) with respect to vectors defining the primitive 1×1 cell. This supercell hosting at full ML coverage 10 molecules is commensurate with the $\sqrt{7} \times \sqrt{3}$ periodicity, as presented in Fig.S1 b), and thus can be used for periodic DFT calculations. Calculating the total energies of the slabs containing $2n$, $n=0..5$ molecules allowed to fit hydrogen-bonding energy as well as van der Waals interaction between molecules and the substrate, under simplification of additive character of the bonds. Fig.S2 a) shows the variation of the bonding energies of molecular chain-like structures with increasing number of molecules, corresponding to the structures presented

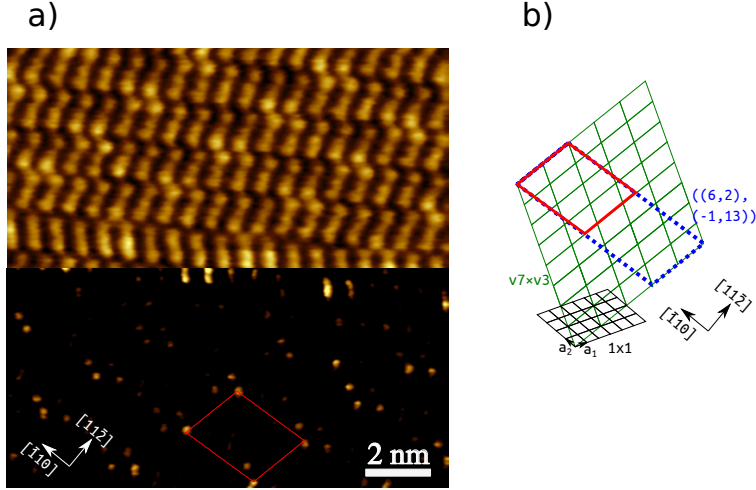


Figure S1: Definition of the supercell for DFT calculations. a) STM image of DPP full monolayer on Si(111)-In($\sqrt{7}\times\sqrt{3}$) with contrast at bottom half enhanced to show a Moire pattern, periodicity of which is marked by a red rhomboid. $U_S = -0.2$ V. b) doubled rhomboid (blue dotted) is commensurate with the $\sqrt{7}\times\sqrt{3}$ structure (green) with matrix $((6,2), (-1,13))$ with respect to vectors defining the primitive 1×1 cell (black).

in Figs. S2 b) and c). In each case the total bonding energy is divided by the number of molecules involved in their formation. The numbers provided above the structure in Figs. S2 b) and c) denote 1) number of molecule-substrate interactions n_S , equal to number of molecules in the slab, 2) number of pairs of hydrogen bonds n_{HB} and 3) number of inter-chain molecule-molecule interactions n_{IC} . The fitted energy in Figs. S2 a) has been obtained as $E_{ads} = E_S + \frac{n_{HB}}{n_S} E_{HB} + \frac{n_{IC}}{n_S} E_{IC}$, where E_X are the corresponding fitted energies. As the superstructure is consistent with the morphology of DT-DPP, we have repeated the same procedure with these molecules to compare the energies. For DP- and DT-DPP, the resultant hydrogen-bonding energies E_{HB} are -0.70 and -0.71 eV per pair of $O\cdots HN$ bonds. The molecule-substrate bonding energies E_S equal to 1.81 and 1.56 eV - these values correspond to the system with two quasi-isolated molecules shown in left panels in Fig. S2 b) and c).

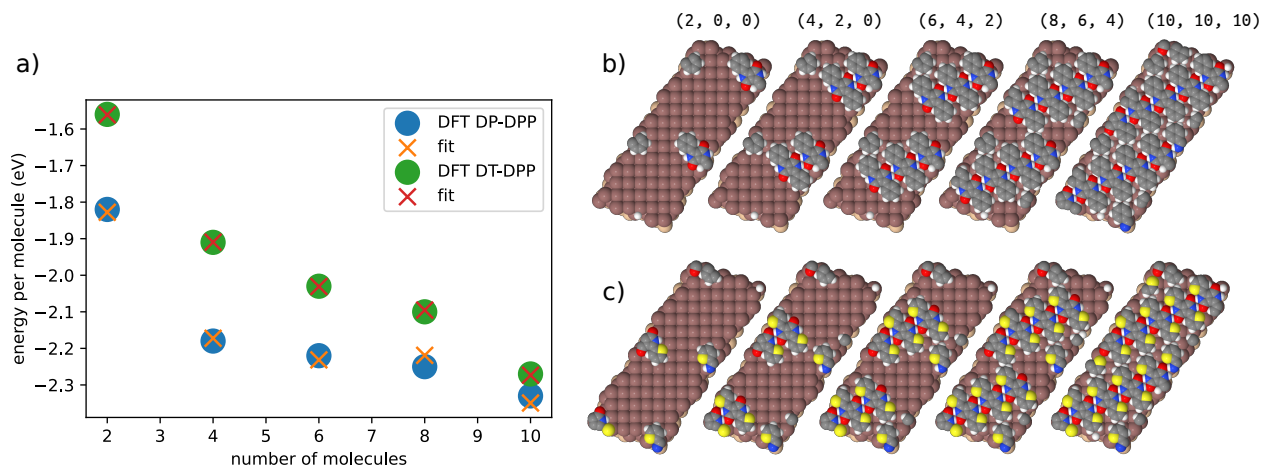


Figure S2: a) Variation of the bonding energies of molecular chain-like structures presented in b) and c) calculated per one molecule - in each case the total bonding energy of the systems is divided by the number of molecules involved in their formation.

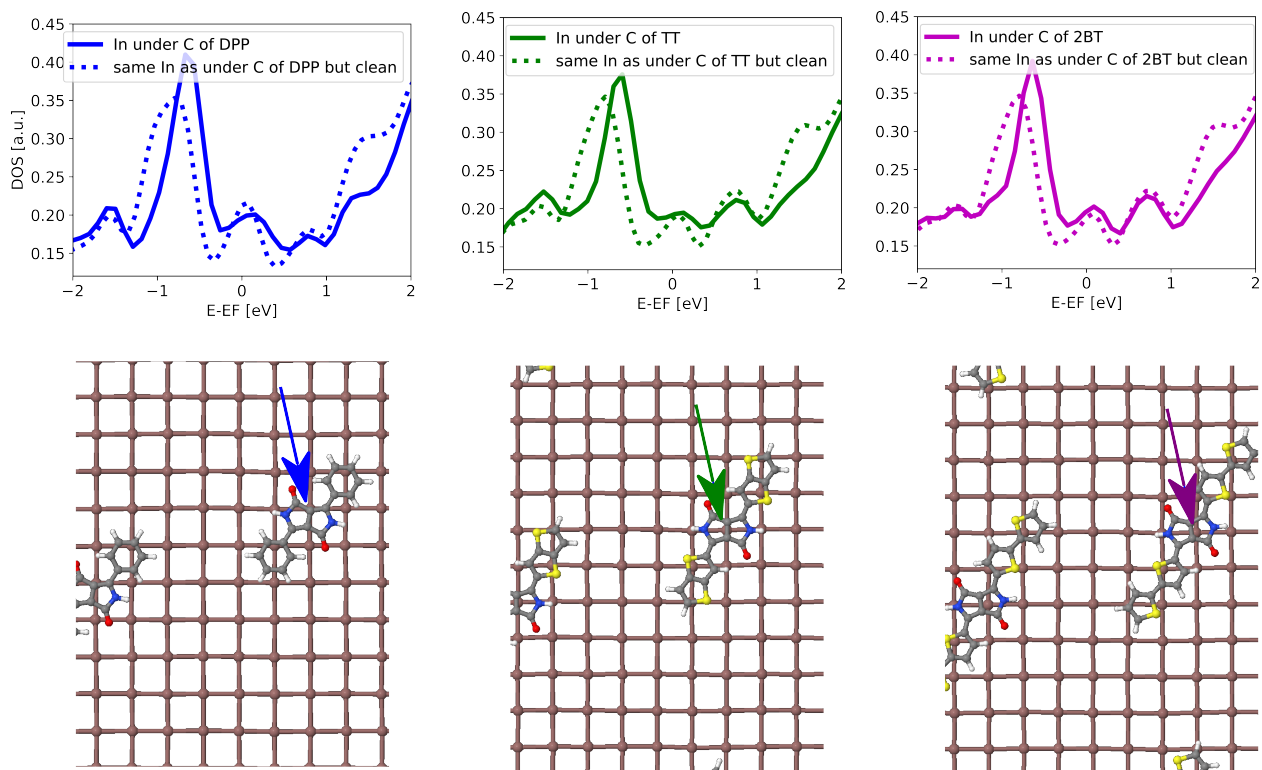


Figure S3: LDOS projected to single atoms below the DP- (left), TT- (middle) and BT-DPP (right) molecules compared to the In atom far from the molecule. The In atoms are indicated by arrows in lower panels.

Additional DOS projected to In atoms

Fig. S3 shows changes of local density of states projected to a surface In atom caused by adsorption of DP- (left), TT- (middle) and BT-DPP (right) molecules. In all cases changes similar to the one caused by DT-DPP (Fig. 3e of the main text) are observed.

In Fig. S4 we present additional projections of DOS to particular atoms of the molecules together with projection to top-most In atoms of the layer in case of all studied DPP derivatives adsorbed on the Si(111)-In($\sqrt{7}\times\sqrt{3}$) .

Fig. S5 shows projections of DOS to In atoms close to and far from DT-DPP molecule (solid lines on left and right side, respectively) compared to projections to the same atoms in absence of molecules (dotted lines). Additional projections to s - and p - orbitals are plotted as well. Most changes due to adsorption are related to s - and p_z - orbitals.

Additional ARPES data

Figs. S6a and c present evolution of valence bands spectra upon deposition of DP- and DT-DPP molecules from pristine Si(111)-In($\sqrt{7}\times\sqrt{3}$) surface to the surface with 60 ML of molecules. In both cases, the characteristic spectrum of the In double layer disappears at 2-3 ML coverage. In Figs. S6b and d the spectra of the thick DPP layers are further compared to DFT calculation of the electronic structures of isolated molecules, obtaining a perfect match. The electronic structures have been calculated using quantum chemical calculations performed by GAMESS (General Atomic and Molecular Electronic Structure System) using the basis system 6-311G+** with the mixed functional B3LYP (Becke-III-Lee-Yang-Parr) as an approximate functional for the exchange correlation energy.

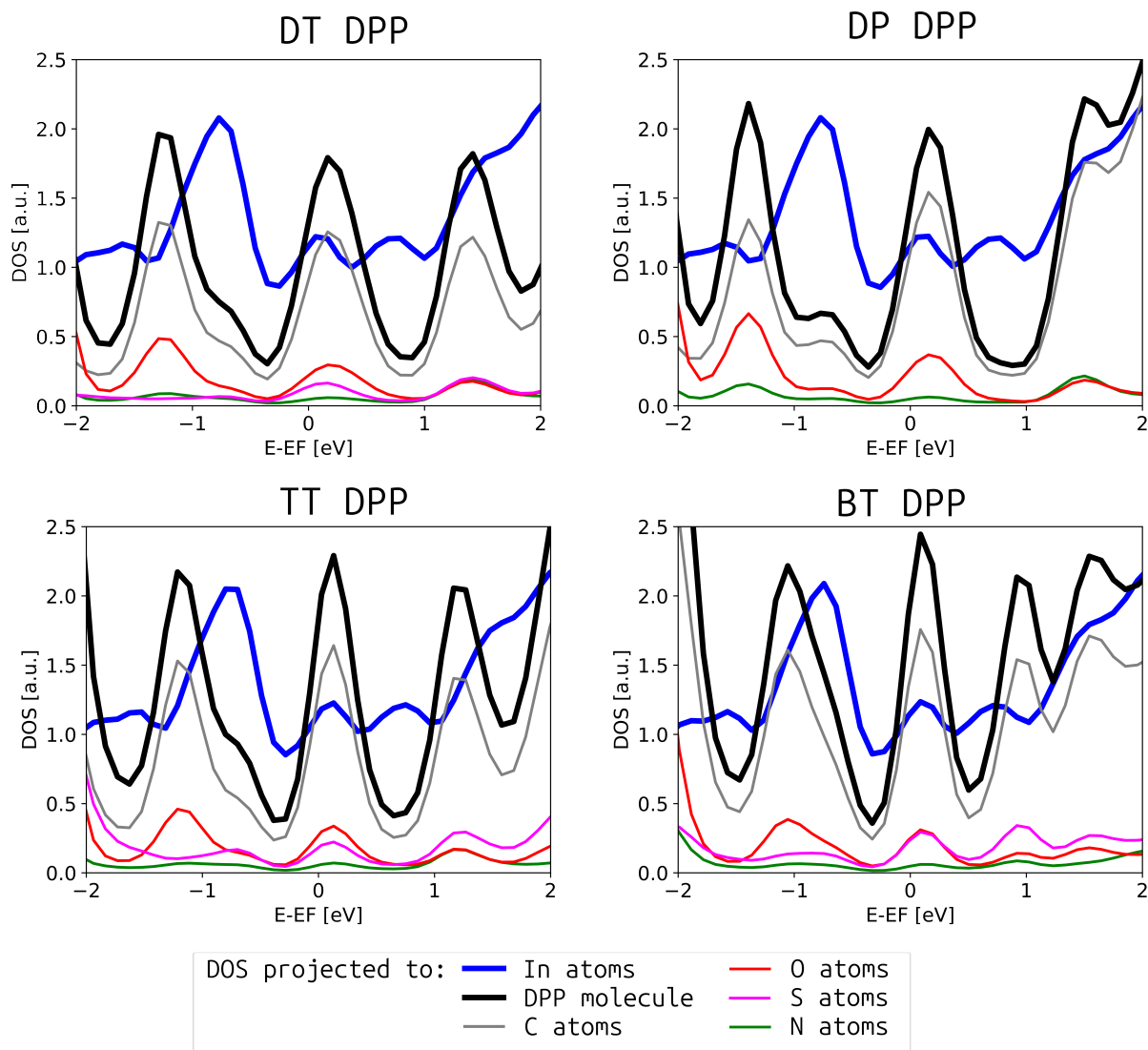


Figure S4: LDOS projected to atoms of indicated DPP molecules and to top-most In atoms for the system of full monolayer of the molecules adsorbed on Si(111)-In($\sqrt{7} \times \sqrt{3}$).

References

1. Iqbal, A.; Jost, M.; Kirchmayr, R.; Pfenninger, J.; Rochat, A.; Wallquist, O. The synthesis and properties of 1,4-diketo-pyrrolo[3,4-C]pyrroles. *Bull. Soc. Chim. Belges* **1988**, *97*, 615–644.
2. Riggs, R. L.; Morton, C. J. H.; Slawin, A. M. Z.; Smith, D. M.; Westwood, N. J.; Austen, W. S. D.; Stuart, K. E. Synthetic studies related to diketopyrrolopyrrole (DPP)

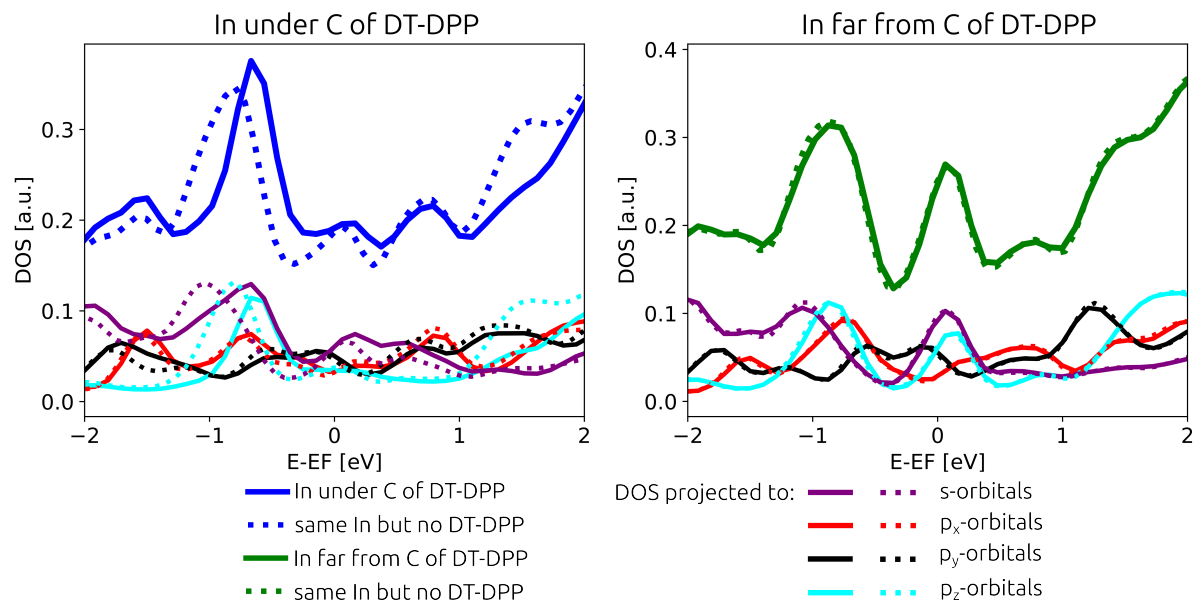


Figure S5: LDOS of Figs. 4e and 4f of the main article with projections to s - and p -orbitals.

pigments. Part 3: Syntheses of tri- and tetra-aryl DPPs. *Tetrahedron* **2005**, *61*, 11230–11243.

- Data, P.; Kurowska, A.; Pluczyk, S.; Zassowski, P.; Pander, P.; Jedrysiak, R.; Czwartosz, M.; Otulakowski, L.; Suwinski, J.; Lapkowski, M.; Monkman, A. P. Exciplex Enhancement as a Tool to Increase OLED Device Efficiency. *J. Phys. Chem. C* **2016**, *120*, 2070–2078.
- Fuller, S. L.; Iddon, B.; A. Smith, K. Thienothiophenes. Part 2.1 Synthesis, metallation and bromine-lithium exchange reactions of thieno[3,2-b]thiophene and its polybromo derivatives. *J. Chem. Soc., Perkin Trans. 1* **1997**, 3465–3470.
- Raimundo, J.-M.; Blanchard, P.; Gallego-Planas, N.; Mercier, N.; Ledoux-Rak, I.; Hierle, R.; Roncali, J. Design and Synthesis of Push-Pull Chromophores for Second-Order Nonlinear Optics Derived from Rigidified Thiophene-Based π -Conjugating Spacers. *J. Org. Chem.* **2002**, *67*, 205–218.

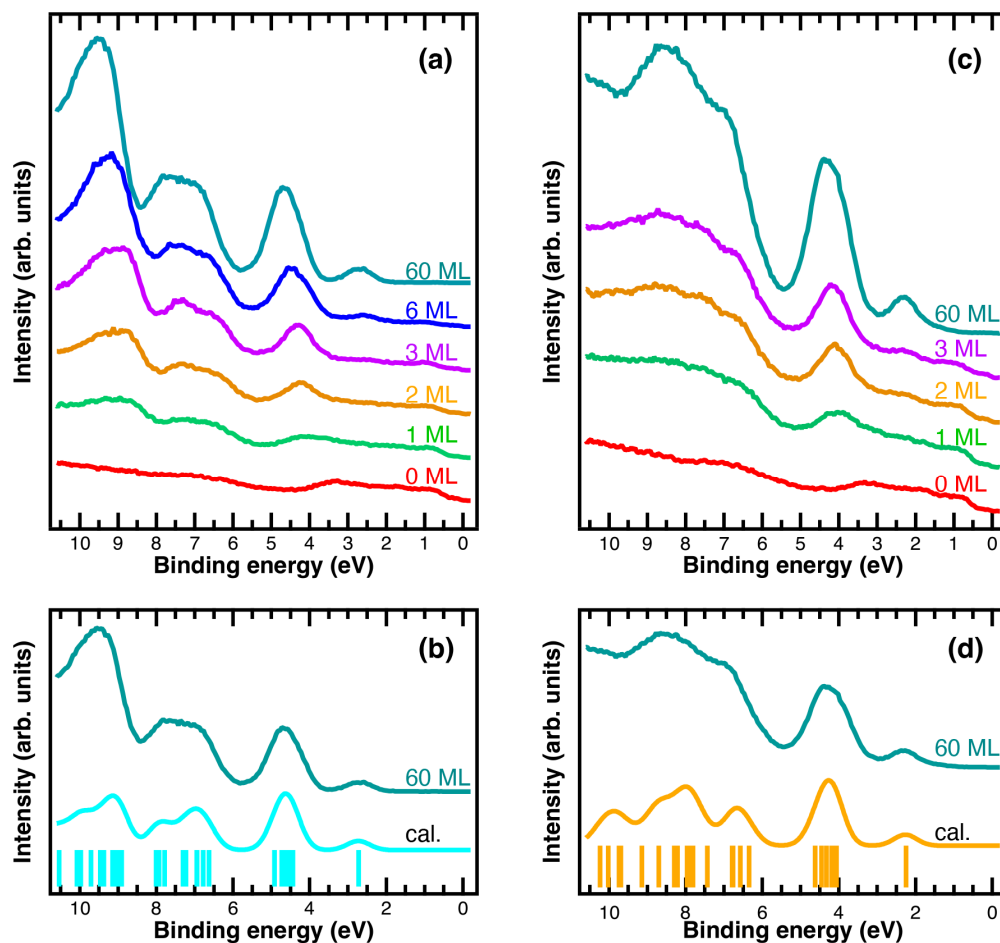


Figure S6: Coverage-dependent valence bands spectra of DP-DPP covered Si(111)-In($\sqrt{7}\times\sqrt{3}$) in (a) and DT-DPP covered Si(111)-In($\sqrt{7}\times\sqrt{3}$) in (c). Comparison between the 60 ML covered samples and the calculated molecular orbitals are shown in (b) and (d) for DP-DPP and DT-DPP, respectively. The vertical bars at the bottom of (b) and (d) indicate the binding energies of the molecular orbitals, and the calculated spectra are obtained by broaden them using a Gaussian function of the FWHM of 0.7 eV.

- Ismail, M. A. An efficient synthesis of 5'-(4-cyanophenyl)-2,2'-bifuran-5-carbonitrile and analogues. *Journal of Chemical Research* **2006**, 2006, 733–737.